Radio-frequency pulse design in parallel transmission under strict temperature constraints

Nicolas Boulant[1], Aurelien Massire[1], Alexis Amadon[1], and Alexandre Vignaud[1]
[1]*Neurospin, CEA, Saclay, Ile de France, France*

Abstract: Although it seems that there is a general consensus that temperature is the true relevant safety parameter, tracking the SAR in MR exams and in RF pulse design has remained the gold standard, probably due to history and simplicity. Given the multi-factorial dependence, indeed this has been a great simplification for handling safety. As RF coil technology, static field intensity and temperature guidelines evolved throughout the years, SAR thresholds on the other hand have pretty much remained identical. Starting from the equilibrium temperature, it was yet shown in Massire et al[1] that after 30 minutes of RF exposure the temperature almost never exceeded 38 °C when the 10-g average SAR did not exceed its limit of 10 W/kg. For significantly shorter sequences, or given the new IEC maximum local temperature guideline of 39 °C issued in 2011, these calculations thus indicated that the recommended SAR thresholds could be quite conservative. Here we investigate numerically a pTX RF pulse design algorithm under strict temperature constraints. The goal is 1) to gain latitude in RF pulse design by possibly relaxing the SAR constraints and 2) to make the MR exam safer.

Methods: The algorithm is based on an iterative procedure where at each iteration, a candidate RF waveform yields a SAR distribution calculated for a generic model[1] which is used as heat source in the Pennes' bioheat equation. Integration of the latter returns the corresponding temperature distribution which is then used to adjust the global and 10-g SAR constraints in order to modify the thermal response accordingly. The updated SAR thresholds are then treated again as hard constraints in the RF pulse design algorithm which returns a new candidate solution and so forth. The magnitude least squares pulse optimization under hard SAR constraints is performed using an active-set algorithm[2] combined with the virtual observation points (VOPs) compression scheme[3]. The example we use to illustrate numerically the algorithm is a simplified 3D time-of-flight sequence of 10 minutes at 7 T, a successful clinical application but also a SAR-demanding sequence at ultra-high field (UHF). The targets are a 90° saturation pulse for a slab located at the top of the brain and a 25° pulse for a thicker and centered slab. In this example, the pulses use a 7 and a 3 k_T-points[4] trajectory respectively and they are played back to back. The sub-pulses are slab-selective and are made of apodized sinc shapes. The pulse design algorithm under strict temperature constraints is briefly summarized as follows:

1. Solve $\min_x f(\boldsymbol{x}) = \left\| \begin{bmatrix} \boldsymbol{A_T} & 0 \\ 0 & \boldsymbol{A_B} \end{bmatrix} \boldsymbol{x} \right| - \begin{bmatrix} \boldsymbol{\theta_T} \\ \boldsymbol{\theta_B} \end{bmatrix} \Big\|_2^2$, s.t. $c_i(\boldsymbol{x}) \leq \mathrm{SAR}_{10g,l}$ $(i = 1, \dots, N_{VOPs})$, $c_G(\boldsymbol{x}) \leq \mathrm{SAR}_{G,l}$, $c_{eye1}(\boldsymbol{x}) \leq \mathrm{SAR}_{eye1,l}$, $c_{eye2}(\boldsymbol{x}) \leq \mathrm{SAR}_{eye2,l}$.
2. Calculate SAR and resulting temperature distributions.
3. Update the SAR limits ($\mathrm{SAR}_{10g,l}$, $\mathrm{SAR}_{G,l}$, $\mathrm{SAR}_{eye1,l}$, $\mathrm{SAR}_{eye2,l}$) according to maximum temperature, rise of core and eye temperatures.
4. Go back to 1 if the decrease of the cost function is significant enough. If the change is negligible, check temperature guidelines. If they are respected, stop. Otherwise, lower SAR thresholds progressively until temperature guidelines are met.

$\boldsymbol{c_i}$, $\boldsymbol{c_{eye}}$, and $\boldsymbol{c_G}$ denote the 10-g SAR values over the VOPs, the 10-g SAR values over the eyes, and the global SAR value respectively. The procedure is not stopped if the temperature constraints are exceeded. Instead, one attempts to maintain them while still making progress (feedback-based approach). The procedure is initialized with the SAR guidelines issued by the IEC. Above $\boldsymbol{\theta_T}$ (= 90°) and $\boldsymbol{\theta_B}$ (= 25°) are the target flip angles (FA) for the top and bottom slabs respectively. Likewise the matrices $\boldsymbol{A_T}$ and $\boldsymbol{A_B}$encode in the same regions the spins'dynamics in the small FA approximation, using the B_1 and ΔB_0 maps (obtained in vivo at 7T, 5 mm isotropic resolution[4]) as well as the k_T-points trajectory.

Results: The FA distributions and final temperature rises are shown in Fig. 1. Eight updates of the SAR thresholds along with implementations of the active-set algorithm could be implemented in less than a minute for this problem in 3D, with a corresponding significant drop of the FA normalized root mean square error (NRMSE). The 10-g and global SAR constraints end up being about three times the SAR recommendations issued by the IEC (except in the eyes where they finally reach 6 W/kg), and yet according to Pennes' bioheat model they do not lead to a violation of the temperature guidelines (rise of core temperature < 0.5°C, T_{max} < 39°C). Specifically, addressing the SAR constraints in the eyes appeared a necessity to make sure the temperature rise did not exceed 1°C at these locations.

Conclusion: A tractable RF pulse design algorithm under strict temperature constraints was reported. If the gain in RF pulse performance obtained by using this method is deemed not worth the risk, this shows on the other hand the possible inadequacy of the SAR constraints for the high field applications utilizing parallel transmission and that gains could likewise be obtained in acquisition time or image resolution. Although further confidence in the thermal models is needed to allow for this flexibility, this work shows that further RF pulse/sequence performance at UHF is within reach.

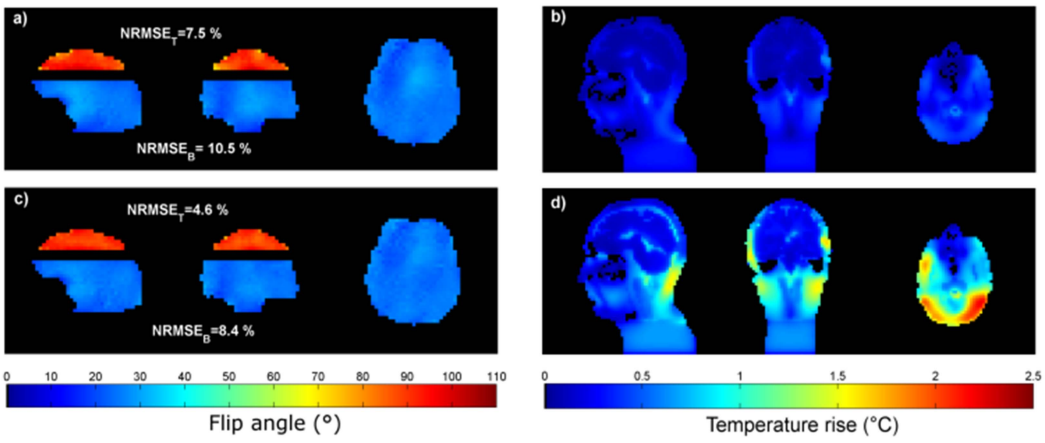

References: 1. A. Massire et al. JMRI 2012;35:1312–1321. 2. A. Hoyos-Idrobo. Submitted to IEEE TMI. 3. J. Lee et al. MRM 2012;67:1566-1578. 4. M. A. Cloos et al. MRM 2012;67:72-80.

Acknowledgments: The research leading to these results has received funding from the European Research Council under the European Union's Seventh Framework Program (FP7/2013-2018) / ERC Grant Agreement n. 309674.

Fig.1: FA distributions and temperature rises before (a b) and after (c d) the SAR updates. The top and bottom slabs can easily be identified in a and c. The NRMSEs in the top and bottom slabs are respectively 7.5 % and 10.5 % before updating the SAR thresholds, 4.6 % and 8.4 % after updating them.